Kinetics of light-induced degradation in *a*-Si : H films investigated by computer modeling

© M.N. Meytin, M. Zeman*¶, B.G. Budaguan, J.W. Metselaar*

Moscow Institute of Electronic Technology,
103498 Moscow, Russia
* Delft University of Technology, DIMES–ECTM,
P.O. Box 5053, 2600 GB Delft, The Netherlands

(Получена 4 октября 1999 г. Принята к печати 15 декабря 1999 г.)

In this work we investigated the stability of *a*-Si : H films under illumination and following recovery in dark at different temperatures. The *a*-Si : H films were fabricated with 55 kHz PECVD and with standard rf 13.56 MHz PECVD. We measured the steady-state photocurrent and the dark current after switchhing off the light source as a function of time. We observed photocurrent degradation and following recovery of the dark current. The kinetics of the photocurrent degradation as well as the dark current recovery demonstrated stretched-exponential behavior.

The results of these straightforward measurements in combination with computer modeling were used to determine the effect of light-induced degradation and thermal recovery on the density of states distribution in the band gap of *a*-Si : H.

We have found that the photocurrent degradation and the corresponding increase in the total defect concentration have different kinetics. The different kinetics were determined also for the dark current recovery and the corresponding decrease in the total defect concentration. The results point out that slow and fast types of defects in *a*-Si : H films control the kinetics of light-induced changes of the defect distribution in the band gap. A model is proposed that relates the origin of the fast and slow metastable defects with the distribution of Si-Si bond lengths.

Introduction

One of the importrant problems limiting application of hydrogenated amorphous silicon (*a*-Si : H) material is the instability of its electronic properties and device performance under light illumination. This phenomenon was observed by Staebler and Wronski [1] in 1977 and since then it has still not been fully explained. The most frequently used method for fabricating *a*-Si : H devices is 13.56 MHz plasma enhanced chemical vapor deposition (PECVD). However, this method is characterized by a low growth rate (0.1–0.2 nm/s). For industrial applications a higher growth rate of *a*-Si : H is desirable while maintaining the device quality properties of the material. The growth rate can be increased by applying higher rf power or vhf frequency, but these layers show inferior electronic properties [2]. Recently it was demonstrated [3] that *a*-Si : H films can be fabricated by 55 kHz PECVD with high growth rate (more than 1 nm/s) and device quality opto-electronic properties. Since these films exhibit microstructural inhomogeneities, we have investigated the stability of these films under illumination and following recovery in dark at different temperatures and compared the results with the 13.56 MHz PECVD *a*-Si : H films.

We observed photocurrent degradation and following recovery of the dark current. The kinetics of the observed degradation and recovery are different for different temperatures. Existing models describe the photocurrent degradation as a process in which the defect concentration in the material increases. These additional defects intoduce metastable states in the band gap of *a*-Si : H and cause a shift of the Fermi level towards midgap [4]. The kinetics of light-induced formation of defects in *a*-Si : H has been investigated in other groups by means of analysis of sub-band gap absorption spectra that change during light soaking [5].

In this work we combined the measurements and computer modeling of photocurrent and dark current in order to investigate the metastable changes of the density of states (DOS) in the band gap of *a*-Si : H during the material degradation and recovery. We used Amorphous Semiconductor Analysis computer program (ASA) developed at the Delft University of Technology [6].

Experimental details

The *a*-Si : H films were fabricated from pure silane by standart 13.56 MHz PECVD and 55 kHz PECVD [7] at the deposition conditions presented in Table 1. The films were deposited on Corning 7059 glass substrate. The aluminum coplanar contacts were deposited for the conductivity measurements. The optical properties of the films were determined by reflection and transmission measurements and double beam photoconductivity measurement.

The measurements of current degradation under illumination were carried out at 50°C, 70°C and 90°C. The samples were illuminated with metal halide lamps with light intensity of 37.5 mW/cm^2. The steady-state photocurrent and the dark

Table 1. The deposition conditions of *a*-Si : H films

Plasma frequency	Pressure, Pa	Power, mW/cm^2	T_s, °C	SiH_4 flow rate, sccm	Deposition rate, nm/s
13.56 MHz	70	15	194	40	0.2
55 kHz	70	50	225	200	0.8

¶ E-mail: m.zeman@its.tudelft.nl

Table 2. The parameters of the photocurrent degradation and the dark current recovery kinetics of *a*-Si : H films measured at different temperatures. The parameters were obtained from the fits to the measured data using stretched-exponential function (Eq. 1)

Samples	Temperature, °C	Degradation			Recovery		
		τ, s	β	E_τ, eV	τ, s	β	E_τ, eV
13.56 MHz PECVD	50	9020	0.61		–	–	
	70	3770	0.43	0.217	7533	0.6	0.38
	90	2550	0.92		3510	0.92	
55 kHz PECVD	70	1602	0.44	0.50	12300	0.94	
	90	362	0.95		5000	0.95	0.44

current after switching off the light source were measured as function of time. Before each degradation-recovery cycle the samples were annealed at 150°C for 30 minutes.

Results

Fig. 1 shows the time change of photocurrent during degradation and of the dark current recovery at 70°C for standard 13.56 MHz and 55 kHz PECVD *a*-Si : H layers.

The behavior of degradation of the photocurrent and the recovery of the dark current is similar to the observed Staebler–Wronski effect (SWE) [8]. In order to deduce the parameters of kinetics of the light-induced degradation and recovery, the measured data of the photocurrent and dark current were normalized and fitted using the stretched-exponential dependence [4] expressed by Eq. 1:

$$\frac{\xi(t)-\xi(\infty)}{\xi(0)-\xi(\infty)} = \exp\left(-\left(\frac{t}{\tau}\right)^{\beta}\right), \qquad (1)$$

where: $\xi(0)$ is the initial value of fitted parameter, $\xi(\infty)$ is the saturated value of fitted parameter, τ is characteristic time, β is the dispersion parameter and t is time. Fig. 2 shows the normalized photocurrent data (dots) for 55 kHz PECVD sample measured at different temperatures and the corresponding fits (lines).

The parameters of stretched-exponential function (τ, β) that were obtained from the fits to the normalized measured data are presented in Table 2. Assuming that the characteristic time τ is thermally activated [9]

$$\tau = \tau_0 \exp(E_\tau / kT), \qquad (2)$$

where τ_0 is the prefactor and E_τ is the characteristic time activation energy, the values of E_τ were calculated for *a*-Si : H films.

Modeling

We applied computer modeling of photocurrent and dark current using the ASA program in order to investigate the effect of light-induced degradation and thermal recovery on the material properties. We based our approach on an assumption that the degradation and recovery processes are mainly determined by metastable changes of the density of states distribution in the band gap of *a*-Si : H. Further we assumed:

a) The time change of the photocurrent and dark current is related to the change in the total defect concentration (N_{db}) and the shift of the defect states distribution in the band gap. The band gap is represented by the mobility gap of *a*-Si : H.

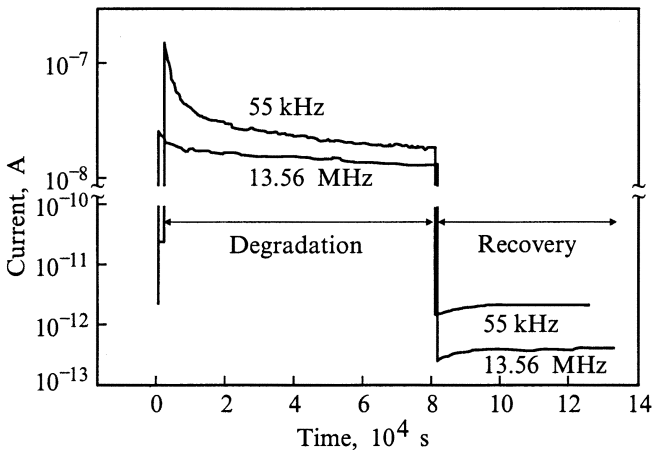

Figure 1. The time change of photocurrent during light-induced degradation and of dark current recovery at 70°C standard 13.56 MHz PECVD and 55 kHz PECVD *a*-Si : H layers.

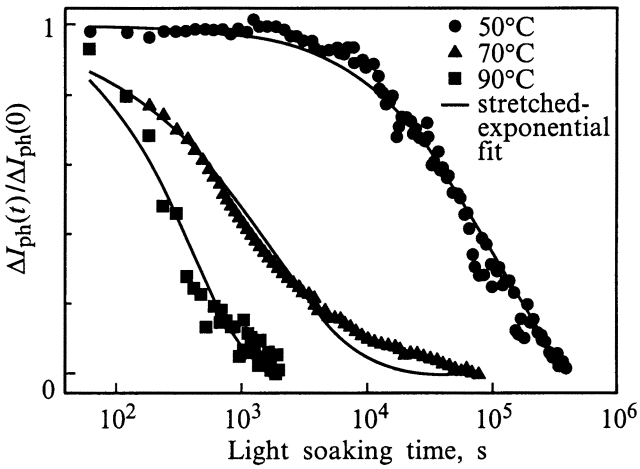

Figure 2. Normalized plot of photocurrent degradation of 55 kHz PECVD *a*-Si : H sample at different temperatures. The lines correspond to stretched-exponential fit.

Table 3. The set of initial input parameters for the simulations. The abbreviations are: CC is capture coefficient, CB (VB) is the mobility edge of conduction (valence) band

General parameters:	55 kHz	13.56 MHz
Tauc optical gap, eV	1.72	1.69
Mobility gap, eV	1.75	1.75
Urbach energy, eV	0.052	0.054
Dielectric constant	11.9	
Electron mobility, 10^{-4} m^2/V · s	10.0	
Hole mobility, 10^{-4} m^2/V · s	2.0	
Tail states parameters:		
DOS at CB mob. edge, m^{-3}/eV	$1 \cdot 10^{27}$	
DOS at VB mob. edge, m^{-3}/eV	$1 \cdot 10^{27}$	
VB tail characteristic energy, eV	0.052	0.054
CB tail characteristic energy, eV	0.027	0.027
CC for neutral states, m^3/s	$7 \cdot 10^{-16}$	
CC for charged states, m^3/s	$7 \cdot 10^{-16}$	
Defect states parameters:		
Standard deviation	0.144	
CC for neutral states, m^3/s	$3 \cdot 10^{-15}$	
CC for charged states, m^3/s	$3 \cdot 10^{-14}$	

b) The defect states are modeled by two equal Gaussian distributions, one representing donor-like defect states ($DB^{+/0}$) and the other acceptor-like defect states ($DB^{+/0}$), that are separated from each other by a correlation energy U (see Fig. 3).

c) Band tails do not change during the degradation and recovery processes. The initial set of input parameters for simulations is presented in Table 3.

The sensitivity study of the influence of the input parameters of the ASA model on the dark- and photocurrent has shown that the dark current is strongly sensitive to the change of the peak position of the Gaussian distribution while the photocurrent is controlled by the total defect concentration. Therefore the data of the dark current recovery were used to determine the kinetics of the shift of the peak of the Gaussian distribution. In this case the energy level $E_{DB}^{+/0}$, which is the peak of the Gaussian distribution of $DB^{+/0}$ states, was used as a variable parameter in simulations. The Fermi level position followed the changes of $E_{DB}^{+/0}$ as $E_F = E_{DB}^{+/0} + U/2$.

The time dependence of the peak position of Gaussian distribution $E_{DB}^{+/0}$ for 13.56 MHz and 55 kHz PECVD sapmles at 70°C is presented in Fig. 4. The time dependence of the peak position was fitted using stretched-exponential function (Eq. 1) and the kinetics parameter τ was determined. The characteristic time τ characterizing the time dependence of the shift of the peak position is in good agreement with the characteristic time τ of dark current recovery. We conclude that the kinetics of dark current recovery is controlled by the shift of the peak position of Gaussian distribution of defect states.

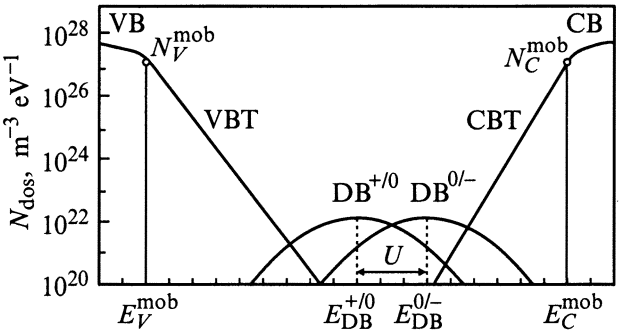

Figure 3. The DOS distribution model used in simulations. Abbreviations: VB (CB) is the parabolic distribution of valence (conduction) band, VBT (CBT) is the exponentially decaying valence (conduction) band tail, E_V^{mob} (E_C^{mob}) is the energy level of VB (CB) mobility edge, and N_V^{mob} (N_C^{mob}) is the density of states at the VB (CB) mobility edge. $E_{DB}^{+/0}$ ($E_{DB}^{0/-}$) is the energy level of the peak of the Gaussian distribution of $DB^{+/0}$ ($DB^{0/-}$) states and U is the correlation energy.

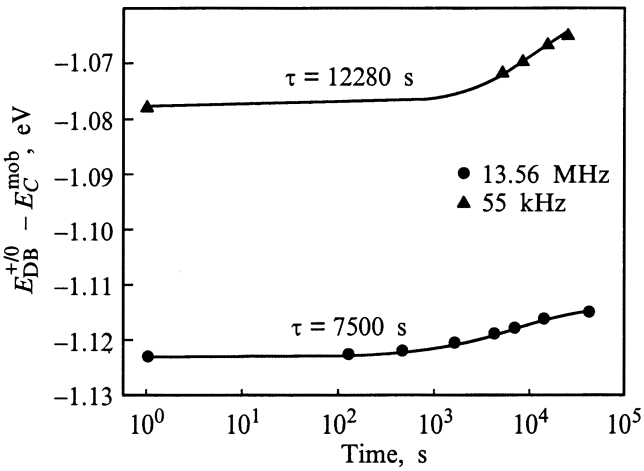

Figure 4. The time dependence of the peak position of Gaussian distribution of defect states during recovery for different *a*-Si:H samples at 70°C. Solid lines correspond to stretched-exponential fit.

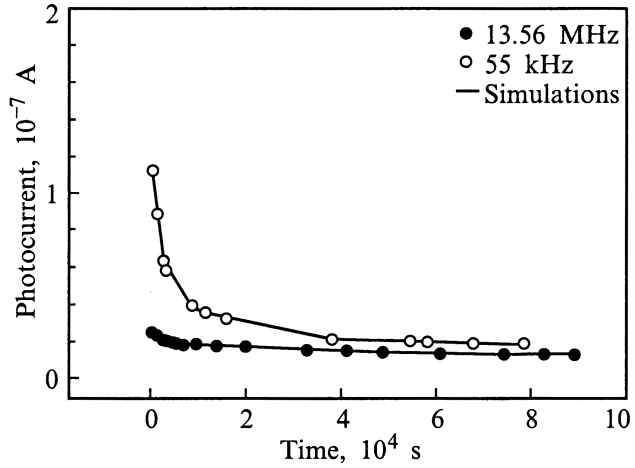

Figure 5. The measured and simulated photocurrent for *a*-Si:H samples at 70°C.

Table 4. The kinetics parameters determined from simulation with the ASA program both for the light-induced degradation and thermal recovery

Samples	Defect generation					Defect annealing				
	τ, s	β	$N_{db}(0)$, cm^{-3}	$N_{db}(\infty)$, cm^{-3}	E_τ, eV	τ, s	β	$N_{db}(0)$, cm^{-3}	$N_{db}(\infty)$, cm^{-3}	E_τ, eV
55 kHz										
$T = 70°C$	16000	0.7	$2.00 \cdot 10^{14}$	$2.00 \cdot 10^{16}$	1.98	1670	0.42	$2 \cdot 10^{16}$	$8.10 \cdot 10^{15}$	0.10
$T = 90°C$	300	0.42	$4.89 \cdot 10^{16}$	$5.50 \cdot 10^{16}$		1380	0.71	$5.56 \cdot 10^{16}$	$5.39 \cdot 10^{16}$	
13.56 MHz										
$T = 70°C$	16730	0.643	$1.55 \cdot 10^{16}$	$2.69 \cdot 10^{16}$	0.26	1600	0.64	$2.71 \cdot 10^{16}$	$2.00 \cdot 10^{16}$	0.03
$T = 90°C$	9900	0.7	$1.44 \cdot 10^{16}$	$1.78 \cdot 10^{16}$		1500	0.7	$1.81 \cdot 10^{16}$	$1.56 \cdot 10^{16}$	

We assume that the kinetics of photocurrent degradation is also controlled by light induced shift of the peak position of Gaussian distribution of defect states and that the kinetics parameters τ and β are the same for both cases. Using this assumption for the peak position of the Gaussian distribution of the defect states we simulated the photocurrent with the ASA program using the total defect concentration as a variable parameter in order to obtain good matching between the measured and simulated values. The time dependence of the measured and simulated photocurrent for *a*-Si:H samples at 70°C is shown in Fig. 5 and the corresponding time dependence of the total defect concentration, N_{db}, in Fig. 6, respectively. The calculated values of the defect concentration demonstrate the stretched-exponential behavior, saturating at large light soaking times (Table 4).

The correlation between the defect concentration N_{db} and the peak position of the Gaussian distribution of the defects during light induced degradation is presented in Fig. 7. As one can see, the shift of the peak position of Gaussian distribution $E_{\mathrm{DB}}^{+/0}$ leads to the increase of the defects concentration N_{db}. The theoretical dependence of the defect density on the energy level of defect in the band gap at equilibrium was calculated according to the known model [4] by the following formula:

$$N_{db} = \left[\frac{N_{v0}E_0kT}{E_0 - kT}\right]\left[\frac{E_0}{kT}\exp\left(-\frac{E_d}{E_0}\right) - \exp\left(-\frac{E_d}{kT}\right)\right], \quad (3)$$

where N_{v0} is density of states at valence band edge, E_0 is Urbach energy, E_d is the position of defect state in the band gap. As one can see the results of modeling are very close to the theoretical dependence at equilibrium state. The deviation between the theoretical calculations using Eq. 3 and the results of modeling exists because in the Eq. 3 only a single defect level was assumed while in modeling the distribution of defects was used. The correlation between N_{db} and peak position of Gaussian distribution is an intrinsic property of *a*-Si:H and is valid both for degradation and annealing processes taking place at the same temperature. This dependence was used for determination of the time change in the defect density during annealing using the calculated data of the peak position during the dark current recovery. The kinetics parameters determined from simulation with the ASA program both for the light induced degradation and thermal recovery are summarized in Table 4.

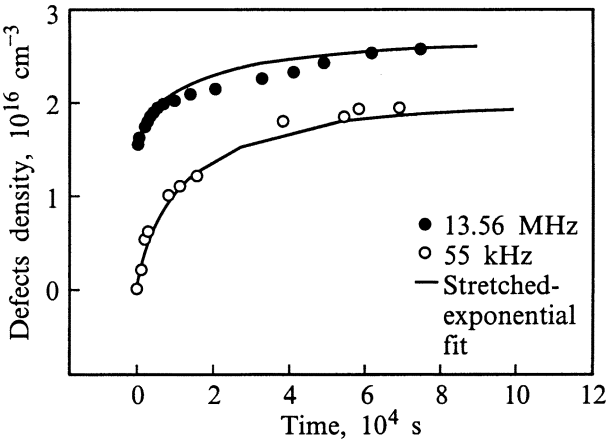

Figure 6. The time dependence of the defect density as determined from the simulations of the photocurrent degradation for *a*-Si:H samples at 70°C. The lines are the fits using the stretched-exponential function.

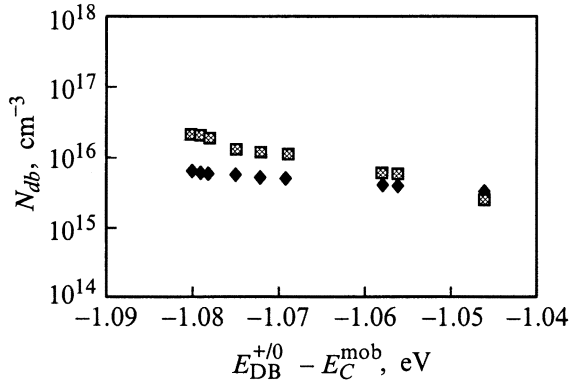

Figure 7. The correlation between the defects density and the peak position of Gaussian distribution during light induced degradation at 70°C for 55 kHz PECVD *a*-Si:H sample. Diamonds correspond to the results of modeling, and squares correspond to the correlation between peak position of Gaussian distribution at equilibrium.

Discussion

As one can see from Table 2, the sample fabricated by 55 kHz PECVD is characterized by higher values of the potential barriers E_τ for the degradation and annealing process. Thus, the use of 55 kHz PECVD results in slowing down the process of photocurrent degradation and dark current recovery, indicating stability improvement of *a*-Si:H films. The analysis of the relation between stability and microstructure of 55 kHz *a*-Si:H is given elsewhere [7]. Here we discuss the degradation and recovery kinetics of *a*-Si:H samples fabricated by different technologies.

The comparison of the measured kinetics parameters, which are listed in Table 2, and the kinetics parameters derived from simulations and presented in Table 4, shows that the photocurrent degradation and the defect creation processes are characterized by different kinetics. The same conclusion holds for the dark current recovery kinetics and the defect annealing kinetics. These phenomena were also observed in SWE experiments, in which the change in defect density was monitored by CPM measurement [10]. Also the activation energy E_τ of characteristic time of the photocurrent degradation and dark current recovery does not correspond to the corresponding E_τ values determined for the defect generation and annealing. This means that the Fermi level shift is controlled by a process characterized with a different energy barrier than an energy barrier involved in a process that controls the formation of additional defects. Two different types of metastable states have been proposed [11,12]: i) the fast defect state, which are responsible for shift of Fermi level during degradation, ii) the slow states, which control the total concentration of the metastable defects. During the degradation the slow defects are characterized by higher activation energy E_τ of the characteristic time than the characteristic time activation energy corresponding to the fast states. According to the data presented in Table 4, during annealing the activation energy E_τ of the characteristic time of the slow defects is less than E_τ of the fast states. Therefore, the slow states should be less stable than the fast ones. The configuration diagram presented in Fig. 8 illustrates the possible processes of creation and annealing of fast and slow defects.

According to known models [4] the creation and annealing of metastable dangling bonds that are associated with dispersive hydrogen diffusion can be presented as the following reaction:

$$\text{Si-H} + \text{Si-Si} \Longleftrightarrow \text{DB} + \text{Si-H-Si}. \qquad (4)$$

The existence of the fast and slow-type defects suggests that there are either different quasi-chemical reactions for defect equilibration process or there is a distribution of Si-Si bond lengths [13]. Assuming that the bond length disorder controls the metastable defect creation and annealing processes in *a*-Si:H the higher values for slow defects formation energy can be explained. The difference between characteristic

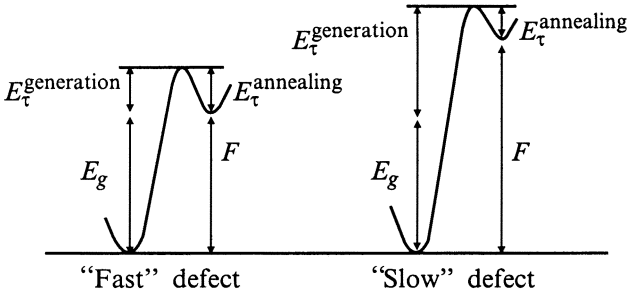

Figure 8. The energy diagram of the fast- and slow-type defects. E_g is the mobility gap, F is the defect formation energy.

energy E_τ of metastable dangling bond creation (Table 4) for standard PECVD film and 55 kHz film suggests that these films can be characterized by different microstructures. A comprehensive study of the relation between light-induced metastability and structural properties of amorphous silicon fabricated by the two techniques is required to fully justify this conclusion.

Conclusions

1. Computer modeling in combination with simple conductivity measurements is an effective tool for the analysis of degradation and annealing processes in amorphous silicon materials.

2. Kinetics of the dark conductivity recovery is controlled by the kinetics of shift of the Fermi level rather than by the kinetics of the change of defect concentration.

3. Kinetics of the photoconductivity degradation is controlled by both the shift of the peak position of the Gaussian distribution of defect states and the change in the defect concentration.

4. It was found that the photoconductivity degradation and the increase in the total defect concentration have different kinetics. The same conclusion holds for the dark conductivity recovery and the decrease in the total defect concentration.

5. Slow and fast types of defects in *a*-Si:H bulk are introduced, which control the kinetics of light-induced changes of the defect distribution in the band gap.

6. It is proposed that the origin of fast and slow metastable defects is connected with a microstructures of the films which influences the distribution of Si-Si bond lengths.

Acknowledgments

This work was supported by the Netherlands Organization for Scientific Research (NWO), grant 047.005.09.96.

References

[1] D.L. Staebler, C. Wronski. Appl. Phys. Lett., **31**, 292 (1977).
[2] P. Roca i Cabarrocas. J. Non-Cryst. Sol., **164–166**, 37 (1993).
[3] B.G. Budaguan, A.A. Sherchenkov, D.A. Stryahilev, A.Y. Sazonov, A.G. Radosel'sky, V.D. Chernomordic, A.A. Popov, J.W. Metselaar. Electrochem. Soc. Symp. (Paris, 1997).
[4] R. Street, K. Winer. Phys. Rev. B, **40**, 6236 (1989).
[5] A.S. Abramov, A.I. Kosarev, P. Roca i Cabarrocas, A.J. Vinogradov. Mater. Res. Soc. Symp. Proc., **420**, 659 (1996).
[6] M. Zeman, J.A. Willimen, L.L.A. Vosteen, G. Tao, J.W. Metselaar. Sol. Energy Mater. and Sol. Cells, **46**, 81 (1997).
[7] B.G. Budaguan, A.A. Aivazov. Mater. Res. Soc. Symp. Proc. (1998) (in press).
[8] C.R. Wronski. *The Staebler–Wronski effect*. In: *Semiconductors and Semimetals*, v. 21, part C, ed. by J.I. Pankove (Academic Press, 1984) p. 347.
[9] J. Kakalios, W.B. Jackson. In: *Amorphous silicon and related materials*, ed. by H. Fritzsche (World Scientific, 1988).
[10] R. Bube, L.E. Benatar, M.N. Grimbergen, D. Redfield. J. Non-Cryst. Sol., **169**, 47 (1994).
[11] Liyou Yang, Liang-Fan Chen. Mater. Res. Soc. Symp. Proc., **297**, 619 (1993).
[12] C. Godet, P. Roca i Cabarrocas. Mater. Res. Soc. Symp. Proc., **420**, 647 (1996).
[13] Qiming Li, R. Biswas. Appl. Phys. Lett., **68**, 2261 (1996).

Редактор В.В. Чалдышев